ESSENTIALS OF PALEOMAGNETISM
LISA TAUXE
UNIVERSITY OF CALIFORNIA PRESS

Errata

After *Essentials of Paleomagnetism* was printed, we detected errors in figures that required correction. The corrected figures follow.

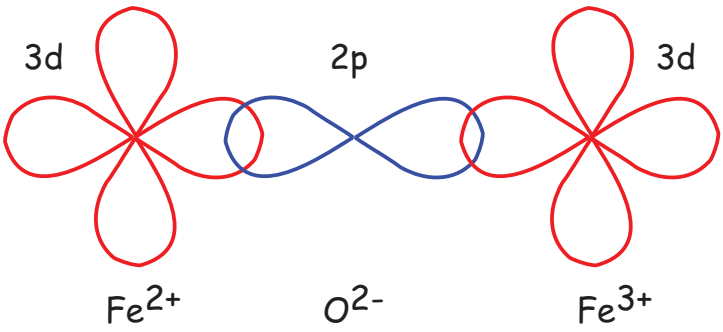

FIGURE 3.6. Exchange energy associated with overlapping orbitals. Example of super-exchange between the $3d$ orbitals of two iron cations through the $2p$ orbitals of the intervening oxygen anion. The two electrons in the $2p$ shells are, by necessity, antiparallel. These are shared by the $3d$ shells; hence, the two cations have antiparallel spins. [Figure redrawn from O'Reilly, 1984.]

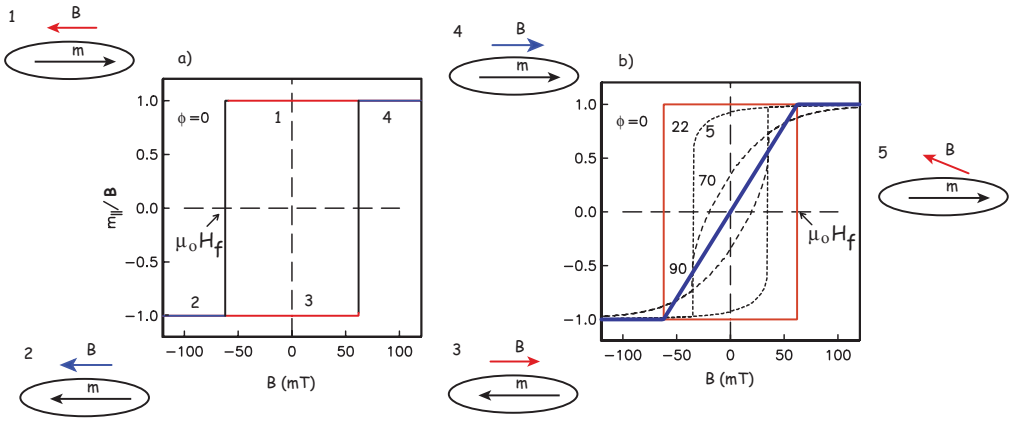

FIGURE 5.4. a) Moment measured for the particle $\phi = 0°$ with applied field starting at 0 mT and increasing in the opposite directions along track #1. When the flipping field $\mu_o H_f$ is reached, the moment switches to the other direction along track #2. The field then switches sign and decreases along track #3 to zero, then increases again to the flipping field. The moment flips, and the the field increases along track #4. b) The component of magnetization parallel to $+B_{max}$ versus B for field applied with various angles ϕ.

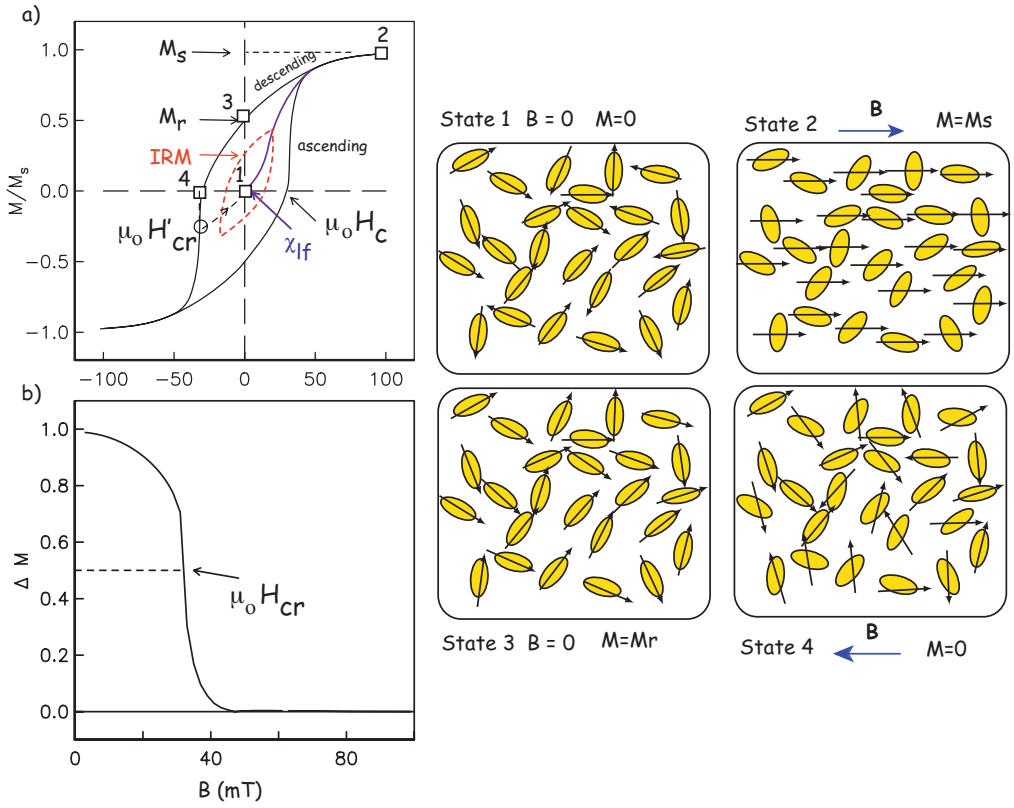

FIGURE 5.5. a) Net response of a random assemblage of uniaxial single-domain particles. Snapshots of magnetization states (squares labeled 1 to 4) for representative particles are shown in the balloons labeled State 1–4. The initial demagnetized state is "State 1." The initial slope as the field is increased from zero is the low-field susceptibility χ_{lf}. If the field returns to zero after some flipping fields have been exceeded, there is a net isothermal remanence (IRM). When all the moments are parallel to the applied field (State 2), the magnetization is at saturation M_s. When the field is returned to zero, the magnetization is a saturation remanence (M_r; State 3). When the field is applied in the opposite direction and has remagnetized half the moments (State 4), the field is the bulk coercive field $\mu_o H_c$. When a field is reached that, when reduced to zero, leaves zero net remanence, that field is the coercivity of remanence (here labeled $\mu_o H'_{cr}$). b) Curve obtained by subtracting the ascending curve in (a) from the descending curve. The field at which half the moments have flipped, leaving a magnetization of one-half of saturation, is another measure of the coercivity of remanence, here labeled $\mu_o H_{cr}$.

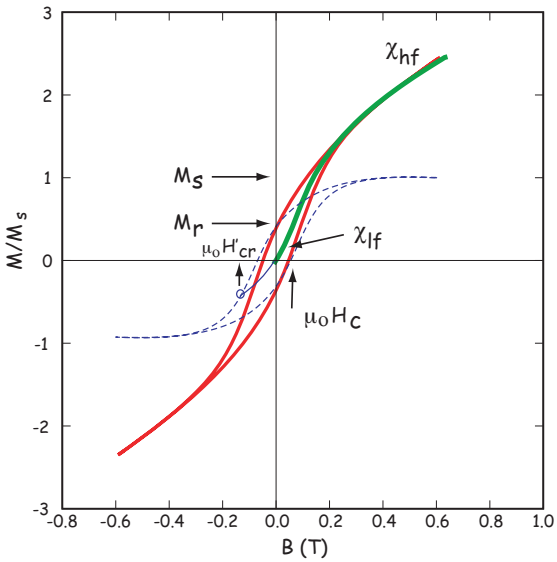

FIGURE 5.6. Heavy green line: initial behavior of demagnetized specimen as applied field ramps up from zero field to a saturating field. The initial slope is the initial or low-field susceptibility χ_{lf}. After saturation is achieved, the slope is the high-field susceptibility χ_{hf}, which is the non-ferromagnetic contribution, in this case the paramagnetic susceptibility (because χ_{hf} is positive). The dashed blue line is the hysteresis loop after the paramagnetic slope has been subtracted. Saturation magnetization M_s is the maximum value of magnetization after slope correction. Saturation remanence M_r is the value of the magnetization remaining in zero applied field. Coercivity ($\mu_o H_c$) and coercivity of remanence $\mu_o H'_{cr}$ are as in Figure 5.5a.

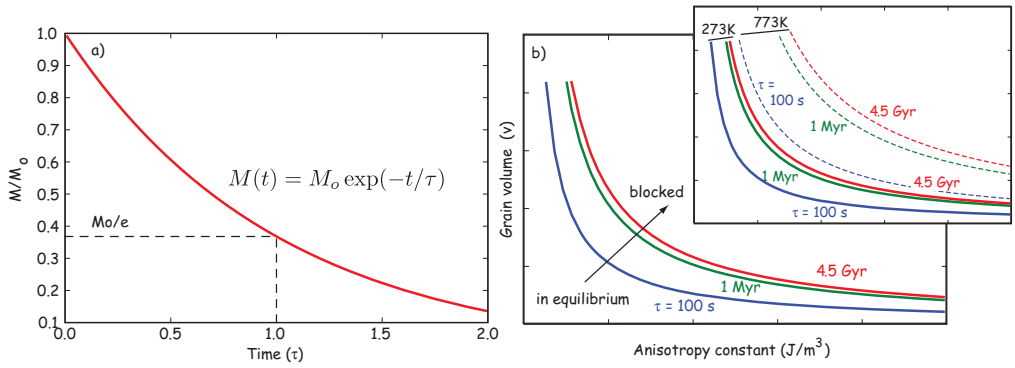

FIGURE 7.2. a) Magnetic relaxation in an assemblage of single-domain ferromagnetic grains. The initial magnetization M_o decays to $\frac{1}{e}$ of its original strength in time τ. b) Relaxation times of single-domain grains on a plot of grain volume, v, against an anisotropy energy constant (K), for a given temperature. Grains with short relaxation times plot toward the lower left and are in equilibrium with the magnetic field (they are superparamagnetic). Grains with long relaxation times plot toward the upper right; their moments are blocked, preserving the magnetization for geologically significant times. Inset shows the effect of temperature on the relaxation time curves, which move toward the right and up with increasing temperature, changing "blocked" remanences to unblocked ones.

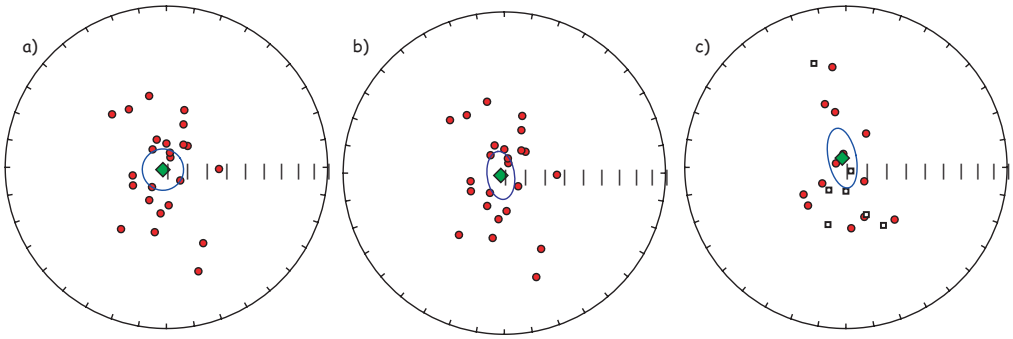

FIGURE 12.2. a) An example of data obtained from a hypothetical equatorial sampling site plotted with the Fisher circle of confidence. The data have been transposed such that the expected direction (0, 0) is at the center of the diagram, and "up" is at the top. b) Same data but with the Kent 95% confidence ellipse. c) Data from (a) with some directions transposed to the antipode; directions plotted with the Bingham 95% confidence ellipse.

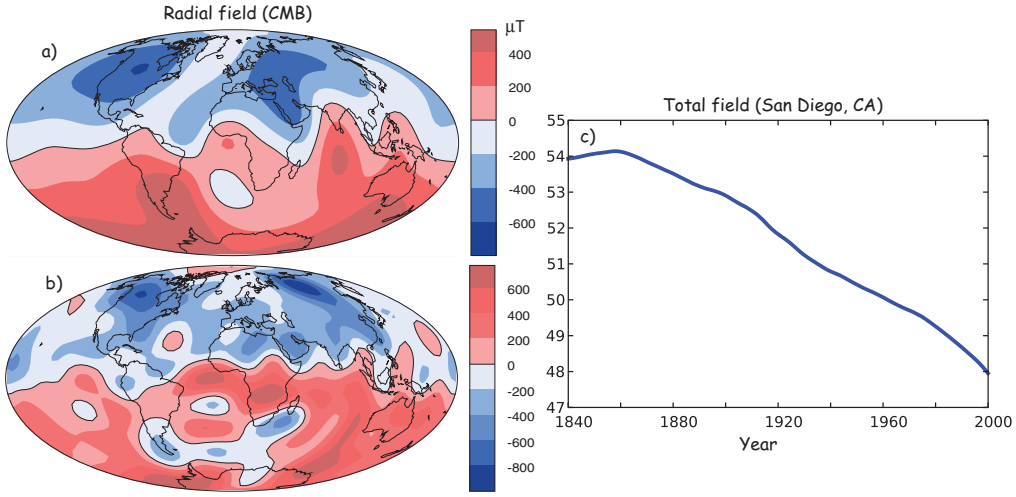

FIGURE 14.4. Maps of the strength of the radial magnetic field at the core–mantle boundary from the GUFM1 secular variation model of Jackson et al. (2000). a) For 1600 CE. b) For 1990. c) Field strength in San Diego, CA, evaluated from the GUFM1 model.

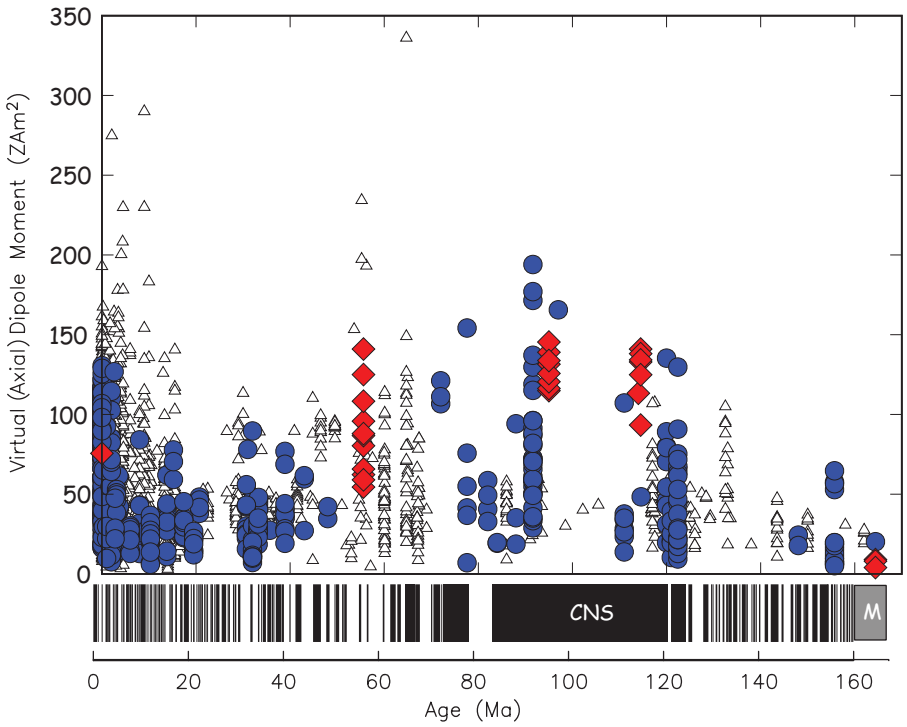

FIGURE 14.15. Summary of data in the PINT06 compilation of Tauxe and Yamazaki (2007) meeting minimum acceptance criteria for the last 200 Ma. Blue dots are submarine basaltic glass data. Red diamonds are single crystal results. Triangles are all other data meeting the same consistency criteria (σ <5% of mean or <5μT); At the bottom is the geomagnetic polarity time scale showing the Cretaceous Normal Superchron (CNS) and the M-sequence of magnetic anomalies. [Figure from Tauxe and Yamazaki, 2007.]